Monoclinic Crystallites in Ethylene Copolymers Detected by Solid-State NMR and X-ray Diffraction

Weiguo Hu*,† and Eric B. Sirota‡

ExxonMobil Chemical Company, 5200 Bayway Drive, Baytown, Texas 77520-2101, and ExxonMobil Research and Engineering Company, 1545 Route 22 East, Annandale, New Jersey 08801-0998

Received February 24, 2003; Revised Manuscript Received April 26, 2003

ABSTRACT: By solid-state NMR and X-ray diffraction techniques, monoclinic crystallites are found to exist in ethylene copolymers with high comonomer content and bulky side groups. In the copolymers, the monoclinic form can nucleate and grow under quiescent conditions, at ambient temperature and pressure. The monoclinic:orthorhombic population ratio increases with comonomer content and cooling rate during crystallization. Compared to the orthorhombic form, monoclinic crystallites have a lower average melting point and possibly a smaller thickness. It is proposed that the formations of the monoclinic crystalline structures in ethylene copolymers and in deformed linear polyethylene share a common mechanism: the monoclinic nuclei are favored by the crystalline−amorphous interface, which increases in importance as the nucleus size decreases at increasing comonomer content or as a result of shear or fast cooling.

Introduction

The monoclinic crystalline phase (MCP) in linear polyethylene has been known to form under several different conditions: shear-induced crystallization or phase transformation, deep undercooling, cryogenic pulverization, and epitaxial crystallization in dilute solution.[1−3] In linear polyethylene, the shear-induced MCP is usually only a minor component of the total crystalline population. The structure of the MCP has been studied by X-ray diffraction, solid-state NMR, and vibrational spectroscopy.[1,4,5]

Several independent solid-state NMR studies also suggested the presence of MCP in ethylene copolymers with high comonomer contents, coexisting with the well-known orthorhombic crystalline phase (OCP).[6−9] It was observed that in ethylene−(dimethylamino)ethyl methacrylate copolymers the MCP:OCP ratio increases with comonomer content and that MCP melts at a lower temperature.[6,7] Since the assignment of solid-state NMR signal to MCP was solely based on the ^{13}C isotropic chemical shift, diffraction data should provide a more rigorous proof of the lattice structure in high-comonomer-content copolymers. It has been reported that deformed ethylene−octene copolymers exhibit MCP diffraction, which was attributed to shear-induced crystallization, similar to linear polyethylene.[10] The experimental data and interpretations leave several unresolved issues of MCP in ethylene copolymers: (1) whether the MCP observed by solid-state NMR can be confirmed by diffraction data; (2) the role of thermal and processing history on the formation of MCP in ethylene copolymers; (3) whether MCP is thermodynamically stable at high comonomer content; (4) whether the presence of MCP is a general phenomenon among all ethylene copolymers.

We attempt to clarify these issues by solid-state NMR and wide-angle X-ray scattering (WAXS) studies of ethylene−butene (EB) and ethylene−octene (EO) copolymers. EB and EO belong to the class of plastomers—ethylene−α-olefin copolymers with high comonomer content (>6 mol %) and low density (<0.9 g/cm^3)—which has been gaining significant practical importance in recent years.[11−14] Despite their commercial significance, their crystal structures have not been well understood. In plastomers, the low levels of crystallinity along with the small size of the crystallites give rise to ill-defined X-ray diffraction peaks which are difficult to assign. In this report, we first identify the MCP structure in EB and EO with both solid-state NMR and diffraction data. Then we discuss its melting and crystallization properties as well as the effect of cooling rate. Finally, we discuss the relationship between the crystalline structures in linear polyethylene, ethylene copolymers, and *n*-alkanes and try to identify a common mechanism for the formation of different crystalline forms.

Table 1. Comonomer Content and Physical State of EB and EO Samples

sample	comonomer content (mol %)	physical state
EB8	7.5	compressed sheet
EB9	9.3	compressed sheet
EB12	12.0	pellet
EB13	12.9	pellet
EB16	15.6	compressed sheet
EB17	16.6	compressed sheet
EB20	19.7	compressed sheet
EO13-1	12.9	compressed sheet
EO13-2	13.0	compressed sheet
EO14	13.7	compressed sheet
EB12/PP blend		pellet

Experimental Section

The samples used in this investigation are shown in Table 1. The nomenclature for the samples has two parts: the first part describes the copolymer type and second the comonomer mole content. An additional number is assigned to each sample where several samples have the same mole percentage. All EB and EO copolymers were made with single-site metallocene catalysts (e.g., ref 15) in a continuous solution process. These polymers usually have a narrow molecular weight distribution and narrow composition distribution. The comonomer content

† ExxonMobil Chemical Company.
‡ ExxonMobil Research and Engineering Company.
* Corresponding author. E-mail: weiguo.hu@exxonmobil.com.

10.1021/ma030132n CCC: $25.00
Published on Web 06/14/2003

of the copolymer samples was determined by either ^{1}H or ^{13}C solution NMR. One blend of polypropylene (made with metallocene catalyst) and EB12 in a 70/30 weight ratio was used in the study. The as-received copolymer samples were either in pellet or compressed sheet form and had been stored at room temperature for at least 1 month.

The solid-state NMR experiments were performed on a Bruker DSX-500 nuclear magnetic resonance (NMR) spectrometer, with a ^{1}H frequency of 500.13 MHz and a ^{13}C frequency of 125.75 MHz. The pulse sequence was a 90° (^{1}H) pulse followed by cross-polarization (CP) and $\pm z$ ^{13}C T_1 filter.[16] The spinning speed was 2−4 kHz, 90° pulse length 4.5 μs, contact time 100−500 μs, and ^{13}C T_1 filter time 1−2 s. Because of the short ^{13}C T_1 of the amorphous regions in the copolymers, most amorphous signals are suppressed by the filter so that the crystalline signals are the prominent peaks on the spectra. All spectra were calibrated with reference to the crystalline signal in high-density polyethylene set at 32.8 ppm. The spectra in the same figure in the Experimental Section were acquired under the same spectrometer conditions and were normalized by the number of scans and sample weight, so that the signal intensity and area can be directly compared to assess the change of crystalline population.

X-ray scattering measurements were performed using a Rigaku 18 kW rotating anode X-ray generator with a copper anode. Cu Kα radiation was selected using a vertically bent graphite monochromator which also focused the beam. The beam size at the sample was determined by slits to be 1 mm horizontal and 2 mm vertical. The sample was located in the center of a Huber two-circle diffractometer. The scattering beam was detected using a Bicron single channel detector behind a horizontal 1 mm wide slit. This gave an arm-zero full-width-half-maximum of ∼0.12°.

Results

Assignment of the Monoclinic Phase. The microstructures of EB and EO copolymers have been well understood on the basis of solution-state ^{13}C NMR studies.[17] At liquid state, different carbons in the copolymer have different ^{13}C T_1 relaxation times due to the mobility difference. For example, for an ethylene−hexene copolymer, end carbons of side branches have the longest ^{13}C T_1, while the methylenes next to the branch points have the shortest ^{13}C T_1.[18] At semicrystalline state, crystalline carbons have much longer ^{13}C T_1 relaxation times than those of amorphous structures due to the reduced mobility. Because many samples in this study have very low crystallinity (<5%), cross-polarization alone is not sufficient to satisfactorily suppress amorphous signals. In addition, the ^{1}H $T_{1\rho}$ values of these crystallites are also quite short (for example, $T_{1\rho}$ for both MCP and OCP in EB12 is about 2 ms), which makes $T_{1\rho}$-based selection of crystalline signal not practical. Therefore, we selected the CP/^{13}C T_1 filter experiment as the main technique to examine the structure and properties of the crystallites.

The CP/^{13}C T_1 spectra of a series of EB copolymers are shown in Figure 1. At low butene content, the prominent signal at 32.8 ppm can be assigned to OCP. At comonomer content of >12 mol %, EB copolymers exhibit two resonances at 33.0 and 34.0 ppm. For sample EB9, which has an intermediate butene content, the signal at 34.0 ppm can be indistinctly seen as a shoulder.

The ^{13}C T_1 relaxation times of sample EB12 were measured to elucidate the nature of the 34.0 ppm peak. At room temperature, the 34.0 ppm signal has a ^{13}C T_1 of ∼10 s, while that of the 33.0 ppm signal is ∼20 s. Note that the relaxation times are nonexponential due to relaxation being partly diffusion-driven, intracrystal

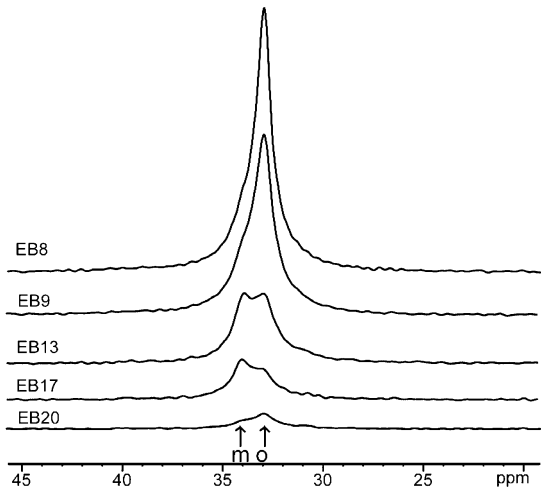

Figure 1. Solid-state CP/^{13}C T_1-filtered NMR spectra of EB copolymers. MCP and OCP signals are labeled "m" and "o", respectively.

T_1 distribution, and intercrystal T_1 distribution. The values reported here are estimated from the final decay slope. The data are consistent with the results by McFaddin et al. for a EO sample with a similar comonomer content (15 mol %).[8] By contrast, for similar EB and EO samples, the uninterrupted amorphous ethylene sequence as well as the amorphous carbons next to the branch points have ^{13}C T_1's of about 0.5 s. The end carbons of side branches in EO have the highest mobility and thus the longest ^{13}C T_1 among all amorphous carbons, ∼1.5 s. However, its signal does not interfere with crystalline signals. The contrast between the ^{13}C T_1 of crystalline and amorphous carbons suggests that the ^{13}C T_1 filter is able to effectively suppress the complication from overlapping amorphous signals and yield useful information about the crystalline phase.

The analysis of the relaxation times of the two phases reveals several characteristics of the 34.0 ppm peak. First, it cannot be from the comonomer structure in the amorphous region, since even the most populous amorphous CH_2 backbone signal has been almost completely suppressed due to the short ^{13}C T_1 (∼0.5 s), and all other amorphous carbons have comparable ^{13}C T_1's. Second, it is from a low-mobility phase, most likely crystalline phase, which gives rise to the ^{13}C T_1 that is much longer than that of the amorphous phase. (It cannot be from carbons in the fast-motion regime, since the fastest carbon at room temperature has a ^{13}C T_1 of only 1.5 s; see previous paragraph.) Third, it is in a different phase than OCP, as judged from their different ^{13}C T_1. Since this peak appears very close to the well-known MCP signal in linear polyethylene, which appears at 34.2 ppm (1.4 ppm downfield of the OCP signal),[4] it can be most reasonably assigned to the monoclinic phase. MCP and OCP exhibit a different isotropic chemical shift since in MCP, the C−C−C planes of adjacent chains are parallel to each other (one chain per unit cell), while in OCP, they are perpendicular (two chains per unit cell). Since the MCP and OCP peaks are overlapping in the NMR spectrum, the possibility of a hexagonal phase (appears at ∼33.4 ppm,[19,20] which is between MCP and OCP singals) cannot be completely excluded. Nevertheless, it would be a minor component compared to MCP and OCP, if it exists at all.

Compared to the MCP signal in linear polyethylene at 34.2 ppm, the MCP peak in copolymers shifts ∼0.2

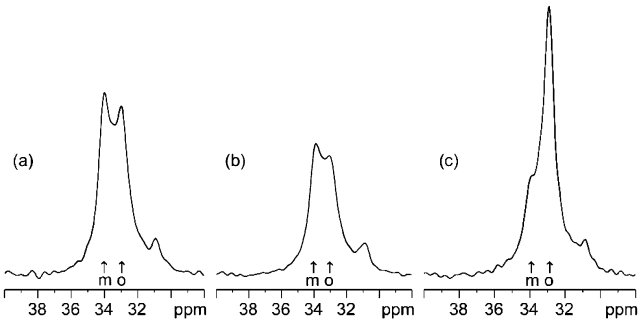

Figure 2. Room temperature spectra of EB12: (a) as-received; (b) melted and quenched in iced water; (c) melted and slowly cooled.

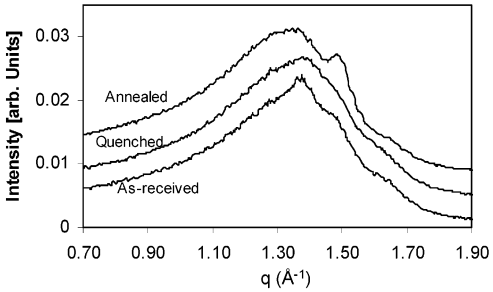

Figure 3. WAXS graph of as-received, iced-water quenched, and slowly cooled EB12 taken at room temperature. The changes of MCP and OCP populations at different thermal histories can be clearly seen.

ppm upfield, toward the OCP signal. The OCP signal also shifts ~0.2 ppm downfield relative to that in linear polyethylene, toward MCP. This may be because the crystalline chains in both phases have significant motional disorder, as also evidenced from the relatively short ^{13}C T_1 values compared with that for high-density polyethylene (usually >100 s). Because of the motional disorder, the C−C−C planes of adjacent chains are probably not strictly perpendicular in OCP, and not strictly parallel in MCP, which likely cause the changes in chemical shifts.[19] The same motional disorder is also the cause of the broadening of both crystalline peaks. A support for this explanation is that, for sample EO13-1 at 0 °C at which chain motion is much more restricted than at ambient temperature, OCP and MCP appear at 32.8 and 34.1 ppm, respectively, which is very close to what is observed in linear polyethylene. At higher temperatures, the splitting decreases.

Comparison of the spectra in Figure 1 indicates that crystallinity decreases quickly with increasing comonomer content. Crystallinity may be estimated on the basis of the spectra in Figure 1, assuming that the cross-polarization efficiencies are the same for all ethylene crystallites and that the error introduced by the ^{13}C T_1 filter is negligible. The crystallinity of EB8 was measured by WAXS to be 20%, and results for other samples can be calculated from the signal area normalized by that of EB8. For example, the crystallinity of EB13 calculated this way is ~8%, of which OCP and MCP each has about 4% (by visual estimation).

It must be noted that there are several potential uncertainties associated with the quantitative aspect of CP/^{13}C T_1 technique. First, since the ^{13}C T_1 of the crystalline carbons is nonexponential and not very long compared to the filter length, the intensity shown on the spectra is only the more ordered part of the crystalline population. Second, different crystalline forms may have a different chain mobility, which may cause their cross-polarization efficiencies be different. Nevertheless, since ^{13}C T_1's of the two phases are not too different, indicative of similar molecular dynamics, and $T_{1\rho}$'s of them are also similar, we can reasonably expect that they have comparable CP efficiencies.

Melting and Crystallization. Figure 2 shows the spectra of EB12 with different thermal histories. The as-received EB12 was produced by extrusion, during which the molten polymer was extruded at high speed, pelletized, and then quenched in water. From Figure 2a, the as-received sample has a comparable amount of OCP and MCP. Figure 2b shows the spectrum of EB12 after it is melted and quenched in iced water (quiescent). In Figure 2c is shown the spectrum of EB12 after being heated to 70 °C to remove most of the crystallinity and then cooled to room temperature at a rate of 1 °C/min. The spectra in Figure 2b,c were both taken 2 h after cooling to room temperature.

Parts a and b of Figure 2 are quite similar in terms of MCP:OCP area ratio, reflecting the similarity of thermal history of the two samples. On the other hand, the freshly quenched sample has less total crystallinity and less-resolved crystalline peaks than in the as-received sample, indicating that a certain portion of crystalline structure requires a longer time to develop. The spectrum of the slowly cooled sample shows a drastic difference in MCP:OCP population ratio, which clearly suggests that cooling rate is critical in controlling the polymorphism. Nevertheless, the shoulder at 34.0 ppm shows that MCP is still able to grow at such a slow cooling rate.

Wide-angle X-ray data of an EB sample, EB12 (as-received, quenched, and slowly crystallized), were acquired (Figure 3) to provide additional support to the NMR assignment. In the as-received sample, three broad crystalline reflections can be seen in addition to the amorphous halo. The reflections at ~1.5 and ~1.65 $Å^{-1}$ are attributed to (110) and (200) reflections of OCP. The sharpest and most prominent reflection at ~1.37 $Å^{-1}$ (corresponding to a d spacing of ~4.6 Å or a Cu Kα diffraction 2θ of ~19.5°) can be reasonably assigned to the (010) reflection of MCP.[1,3,10] The MCP (200) reflection partially overlaps with the OCP (200) reflection.

After the EB12 sample is annealed at 60 °C for 2 h, slowly cooled (by turning off the oven and leaving the sample inside, with an estimated cooling rate of <1 °C/min), and stored at room temperature for 4 days, noticeable differences are seen in the WAXS pattern (see Figure 2). The orthorhombic (110) reflection significantly increases, while the monoclinic (010) reflection almost disappears. This is consistent with the solid-state NMR observation for the same sample undergoing a similar treatment (Figure 2c).

The middle trace of Figure 3 shows the diffraction pattern of sample EB12 which was melted and quenched in iced water. The reflections at ~1.37, ~1.5, and ~1.65 $Å^{-1}$ become very difficult to recognize and, if they do exist, are lower than those in the as-received sample. This is again consistent with the NMR observations in Figure 2.

Because of the significant amount of dynamic and static disorders in these crystallites, as evidenced from the broad line widths of WAXS peaks, the structures seen on the WAXS pattern are likely only more ordered portion of the crystalline population. On the other hand, because of the limitations of the NMR techniques

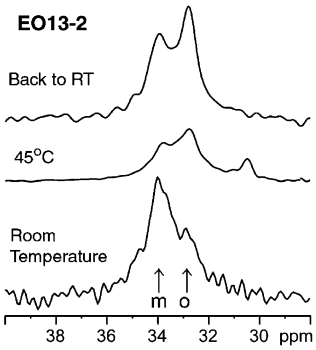

Figure 4. Variable-temperature spectra of EO13-2.

employed, as discussed above, the signals in the NMR spectra also do not represent all the crystallinity. Nevertheless, the directional agreement of WAXS and solid-state NMR data on the change of structure as a function of thermal history supports the existence of MCP in EB copolymers. The reflection at 1.37 $Å^{-1}$ in ethylene copolymers of high comonomer content has been repeatedly reported before; however, its nature was not clearly understood. It was often assigned as a part of the amorphous halo or a partially ordered mesophase with unknown lattice structure. On the basis of the experimental data discussed above as well as in the literature, the reflection can now be assigned to the monoclinic structure.

To further understand the thermal properties of MCP in the copolymers, variable-temperature spectra for EO13-2 were obtained, as seen in Figure 4. At room temperature, MCP has a much larger population than OCP. Comparing the spectra at room temperature (before heating) and at 45 °C, two changes are clearly visible: (1) intensities of both crystalline signals decrease with increasing temperature, indicating a gradual melting of both phases; (2) MCP signal intensity decreases faster than that from OCP, suggesting that the former has a lower average melting point. This agrees with the observation for several other plastomer samples (spectra not shown) as well as ethylene−(dimethylamino)ethyl methacrylate copolymers.[6] We also compared spectra for EO13-1 at room temperature and at 0 °C, which shows that MCP population increases much more significantly than OCP at decreasing temperature. This is consistent with the finding at elevated-temperature experiments. It should be noted that these comparisons are based on the assumption that the CP efficiencies are similar for the two crystalline forms and at different temperatures.

The sample was then slowly cooled back to room temperature in the NMR spectrometer by turning off the heater (with an estimated cooling rate of 4 °C/min), and its spectrum was acquired 2 h later. From Figure 4, the relative population of the two crystalline forms becomes very different from that before heating, similar to the change seen in Figure 2. The as-received EO13-2 sample was prepared by compression molding, during which the molten polymer spreads out upon pressing and then cools at a rate of 20 °C/min. The difference in cooling rate is most likely the cause of the MCP:OCP area ratio difference for as-received and slowly cooled samples.

It has been observed that the ethylene crystal thickness is closely related to its ^{13}C T_1 relaxation time[21] and melting point (T_m).[22] These correlations may not be quantitatively applicable to compare different crystalline forms such as MCP and OCP. Nevertheless, assuming the correlations do apply to both modifications, both ^{13}C T_1 and melting point observations would suggest that MCP crystallites are thinner than OCP. The observation that MCP:OCP ratio increases with comonomer content, indicating that MCP is easier to form from short ethylene sequences than is OCP, supports this conclusion. The coexistence of the two crystalline forms may be interpreted as the result of a distribution of ethylene sequence lengths in the copolymers: longer ethylene sequences tend to crystallize into OCP (high T_m), while shorter ones into MCP (lower T_m).

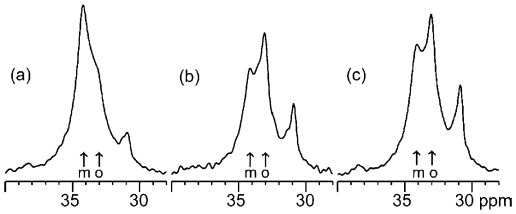

Figure 5. Room-temperature spectra of EO13-1: (a) as-received sample; (b) 2 h after slowly cooled to room temperature from 65 °C; (c) 3 days after slowly cooled to room temperature from 65 °C. The signal at 31 ppm is from the amorphous CH_2 backbone carbons that was not completely suppressed.

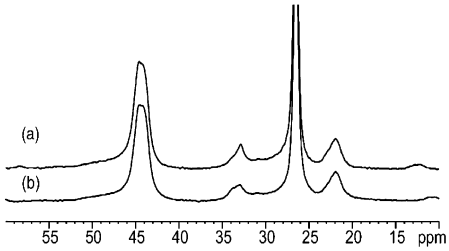

Figure 6. Room temperature spectra of a PP/EB12 blend: (a) slowly cooled from 65 °C; (b) as-received. The small signals at 33−34 ppm are from ethylene crystallites. The signals at 44, 27, and 22 ppm are from crystalline polypropylene.

The spectra of sample EO13-1 at three different states are shown in Figure 5: (a) as-received, (b) 2 h after slowly cooled from 65 °C to room temperature, and (c) 3 days after cooled from 65 °C to room temperature. At 65 °C, EO copolymers at such a composition is usually completely melted.[23] The complete removal of MCP crystallites at 65 °C was verified by a CP/^{13}C T_1 experiment, which shows no MCP signal. Figure 5b shows that the MCP crystallites can both nucleate and grow during slow cooling, agreeing with the observation in Figure 2c. Comparison of parts b and c of Figure 5 indicates that both MCP and OCP can slowly grow at room temperature.

One of the major applications of plastomers is in blends with polypropylene (PP). Therefore, it would be interesting to examine the structure of the plastomer crystallites in a PP/plastomer blend. Figure 6b shows the CP/^{13}C T_1 spectrum of an as-received PP/EB12 blend. At the butene composition of 12 mol %, the two components are immiscible.[24] The sample was prepared by extrusion during which the pellets were quenched in water, thus with a fast cooling rate. Although the two crystalline peaks at 32.8 and 34.0 ppm are not well resolved, it is clear that these two signals are present with comparable intensities. After heated to 65 °C and slowly cooled to room temperature, the MCP intensity significantly decreases, while OCP becomes more populous. This is again in good agreement with the observa-

tions for neat plastomers (Figures 2−5), indicating that the crystallization behaviors of OCP and MCP in the blend are very similar to the case in neat polymers.

Discussion

Relationship between Chain Packing and Crystal Thickness in Polyethylene and *n*-Alkanes. Comparison of the crystalline structure of polyethylene and *n*-alkanes can yield interesting insights to the mechanism of polymorphism in ethylene homopolymer and copolymers. Before making the comparison, it should be noted that the unit cell geometry and local packing are different for polyethylene and *n*-alkanes. In polyethylene, the monoclinic phase contains one chain per unit cell, with C−C−C planes of adjacent chains parallel to each other ("parallel packing"). On the other hand, the orthorhombic phase contains two chains per unit cell and has perpendicular (herringbone) packing. In *n*-alkanes, the orthorhombic and monoclinic phases (with orthorhombic subcell) contain two chains per subcell (perpendicular packing), while the triclinic phase contains one chain per subcell (parallel packing).

It has been observed that shorter *n*-alkanes (n-C_nH_{2n+2} with $6 \le n$ (even) < 26) have parallel packing, similar to MCP in polyethylene, while longer chains ($26 \le n$ (even) ≤ 100) have herringbone packing, like OCP.[4] This seems to suggest a trend that holds for both ethylene copolymers and *n*-alkanes: smaller nuclei tend to form parallel packing (one chain per cell), while larger nuclei tend to form perpendicular herringbone packing (two chains per cell). Such a commonality may be interpreted by the hypothesis that the interior of the crystal energetically favors perpendicular herringbone packing, while the surface favors parallel packing. This would explain the different crystalline structure at different thickness or chain length.

Relationship between the Monoclinic Crystalline Phase in Linear Polyethylene and Ethylene Copolymers. Summarizing the findings of the present report and in the literature, it is reasonable to rationalize that the presence of MCP in ethylene copolymers is a common phenomenon, as long as the comonomer content is high (>9 mol %) and the side group in the copolymer is bulky. Ethylene−propylene copolymers (EP) do not satisfy the second criterion: a methyl group can be incorporated in crystallites due to its small size.[20,25,26] The methyl groups in the crystallites drive the change of the orthorhombic lattice toward a hexagonal/rotator phase instead of the MCP phase.[19]

The concept that the crystalline−amorphous interface favors MCP while the interior of crystal favors OCP seems to suggest that the monoclinic structures in deformed linear polyethylene and in high-comonomer-content ethylene copolymers have a common mechanism of formation. In linear polyethylene, crystallites are thick and the interfacial effect is small; thus, OCP is thermodynamically preferred. Upon strong shear, the lamellar structure is destroyed and chains are recrystallized, resulting in many small crystallites, some of which are so small that they gradually melt at room temperature.[1] Such small crystallites have a large interfacial area and thus tend to be MCP.

In ethylene/olefin copolymers, crystallites are much thinner than in unoriented linear polyethylene; thus, the relative contribution of the interface to the energetics of crystallites is much greater. As a result, the MCP population would be much more favored (except for EP copolymers). Fast cooling causes nucleation at lower temperature; thus the critical nucleus is smaller, which tends to be MCP. This would explain the fact that MCP is more populous in quenched samples. Similar to linear polyethylene, shear or orientation during crystallization may also enhance MCP population in the copolymers.

Finally, we would like to speculate the mechanism by which the interface or surface would favor formation of parallel packing. For *n*-alkane crystals, parallel packing may give crystal surfaces on which the end groups are more evenly distributed and less crowded. For polymer crystals, it could be related to the motion of the segments on the amorphous side of the interface. The reorientation motion of the segments just outside the crystallites is highly confined and may not be axially symmetric with respect to the chain axis. Therefore, parallel packing would allow adjacent chains to move collectively, while perpendicular packing could result in more interference between the motions of adjacent chains. As a result, interface of parallel-packing crystal could have a lower free energy.

Conclusion

Monoclinic crystallites are found to exist at significant quantity in ethylene copolymers with high comonomer content and bulky side groups. They have a lower melting point and are less favored to form during slow cooling but are significantly enhanced under fast cooling conditions. On the other hand, the crystallization into the orthorhombic form is favored during slow cooling. It is proposed that the monoclinic structures of ethylene copolymers and in deformed linear polyethylene share the same mechanism: the crystalline−amorphous interface is a crucial contribution to the stability of the monoclinic phase. Shear, fast cooling, and bulky comonomer increase the contribution of the interface to the free energy, thus favoring the monoclinic form.

References and Notes

(1) Russell, K. E.; Hunter, B. K.; Heyding, R. D. *Polymer* **1997**, *38*, 1409−1414.
(2) Wittmann, J. C.; Lotz, B. *Polymer* **1989**, *30*, 27−34.
(3) Lovinger, A. J.; Belfiore, L. A.; Bowmer, T. N. *J. Polym. Sci., Part B: Polym. Phys.* **1985**, *23*, 1449−1466.
(4) VanderHart, D. L.; Khoury, F. *Polymer* **1984**, *25*, 1589−1599.
(5) Siesler, H. W. *Makromol. Chem.* **1989**, *190*, 2653−2663.
(6) Lin, W.; Zhang, Q.; Yang, G.; Chen, Q. *J. Mol. Struct.* **2002**, *602*−*603*, 185−190.
(7) Luo, H.-J.; Chen, Q.; Yang, G.; Xu, D. *Polymer* **1998**, *39*, 943−947.
(8) McFaddin, D. C.; Russell, K. E.; Wu, G.; Heyding, R. D. *J. Polym. Sci., Part B: Polym. Phys.* **1993**, *31*, 175−183.
(9) Glowinkowski, S.; Makrocka-Rydzyk, M.; Wanke, S.; Jurga, S. *Eur. Polym. J.* **2002**, *38*, 961−969.
(10) Vanden Eynde, S.; Rastogi, S.; Mathot, V. B. F.; Reynaers, H. *Macromolecules* **2000**, *33*, 9696−9704.
(11) Mouzakis, D. E.; Mader, D.; Mulhaupt, R.; Karger-Kocsis, J. *J. Mater. Sci.* **2000**, *35*, 1219−1230.
(12) Portnoy, R. C. *J. Appl. Med. Polym.* **1999**, *3*, 39−43.
(13) Dharmarajan, N.; Yu, T. C.; Metzler, D. K. In *Annual Technical Conference*; Society of Plastics Engineers, 2001; Vol. 59 (Vol. 2), pp 1694−1698.
(14) Yu, T. C. *Polym. Eng. Sci.* **2001**, *41*, 656−671.
(15) Rix, F. C. PCT International Application WO 0024793, 2000.
(16) Torchia, D. A. *J. Magn. Reson.* **1978**, *30*, 613−616.
(17) Randall, J. C. *J. Macromol. Sci.* **1989**, *C29*, 201−317.
(18) Axelson, D. E.; Mandelkern, L.; Levy, G. C. *Macromolecules* **1977**, *10*, 557−558.
(19) Hu, W.; Srinivas, S.; Sirota, E. B. *Macromolecules* **2002**, *35*, 5013−5024.

(20) Bracco, S.; Comotti, A.; Simonutti, R.; Camurati, I.; Sozzani, P. *Macromolecules* **2002**, *35*, 1677−1684.
(21) Axelson, D. E.; Mandelkern, L.; Popli, R.; Mathieu, P. *J. Polym. Sci., Polym. Phys. Ed.* **1983**, *21*, 2319−2335.
(22) Wunderlich, B. *Macromolecular Physics*; Academic Press: New York, 1980; Vol. 3.
(23) Vanden Eynde, S.; Mathot, V. B. F.; Koch, M. H. J.; Reynaers, H. *Polymer* **2000**, *41*, 4889−4900.
(24) Yamaguchi, M.; Miyata, H.; Nitta, K.-H. *J. Appl. Polym. Sci.* **1996**, *62*, 87−97.
(25) Perez, E.; VanderHart, D. L.; Crist, B.; Howard, P. R. *Macromolecules* **1987**, *20*, 78.
(26) Hosoda, S.; Nomura, H.; Gotoh, Y.; Kihara, H. *Polymer* **1990**, *31*, 1999.

MA030132N